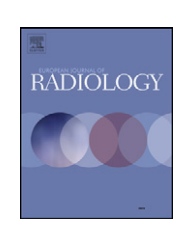
ELSEVIER

Contents lists available at SciVerse ScienceDirect

European Journal of Radiology

journal homepage: www.elsevier.com/locate/ejrad



Mucosa-associated lymphoid tissue lymphoma of the salivary glands: MR imaging findings including diffusion-weighted imaging

Hiroki Kato^{a,*}, Masayuki Kanematsu^{a,b,1}, Hiroo Goto^{c,2}, Keisuke Mizuta^{d,3}, Mitsuhiro Aoki^{d,3}, Bunya Kuze^{d,3}, Yoshinobu Hirose^{e,3}

- ^a Department of Radiology, Gifu University School of Medicine, 1-1 Yanagido, Gifu 501-1194, Japan
- ^b High-level Imaging Diagnosis Center, Gifu University Hospital, 1-1 Yanagido, Gifu 501-1194, Japan
- ^c Department of Radiology, Gifu Red Cross Hospital, 36-3 Iwakura-cho, Gifu 501-1194, Japan
- d Department of Otolaryngology, Gifu University School of Medicine, 1-1 Yanagido, Gifu 501-1194, Japan
- ^e Department of Pathology, Gifu University School of Medicine, 1-1 Yanagido, Gifu 501-1194, Japan

ARTICLE INFO

Article history: Received 18 November 2011 Received in revised form 22 December 2011 Accepted 24 December 2011

Keywords: Mucosa-associated lymphoid tissue lymphoma MALT Salivary gland Diffusion-weighted imaging

ABSTRACT

Purpose: The purpose of this study was to describe MR findings including diffusion-weighted (DW) imaging findings in patients with mucosa-associated lymphoid tissue (MALT) lymphoma of the salivary glands.

Materials and methods: Ten patients with histologically proven MALT lymphoma of the salivary glands were included. All patients underwent 1.5-T MR imaging, six of the ten underwent DW imaging, nine underwent CT, and eight ¹⁸F-fluorodeoxyglucose (FDG) PET/CT. MR images were reviewed for numbers, locations, sizes, MR imaging characteristics, and apparent diffusion coefficients (ADCs). Calcium deposition and maximum standardized uptake values (SUVmax) were also assessed.

Results: Twenty-six tumors, ranging in number from 1 to 5 (mean, 2.6), were identified. Nine patients had tumors in the parotid glands and one in the submandibular glands. Tumors were found bilaterally in 7 patients and unilaterally in three. Tumors ranged in size from 0.6 to 5.5 cm (mean, 1.8 cm). Ten (38%) tumors had intratumoral cystic formations and 8 (31%) had ill-demarcated margins. DW images showed hyperintensity with extremely low ADCs (range, 0.48–0.82 [\times 10⁻³ mm²/s]; mean, 0.64) for solid components of all 19 tumors in the 6 examined patients. Calcium deposition was found in one (4%) tumor on CT. SUVmax variously ranged from 1.3 to 17.7 (mean, 6.3).

Conclusion: Salivary gland MALT lymphomas were often found bilaterally and were occasionally accompanied by intratumoral cystic formations and ill-demarcated margins. DW imaging may play a supplementary role in the diagnosis of lymphoma, because it showed restricted water molecule diffusion, whereas PET/CT showed indeterminate findings.

© 2012 Elsevier Ireland Ltd. All rights reserved.

1. Introduction

Malignant lymphoma arising from mucosa-associated lymphoid tissue (MALT) was first described by Isaacson and Wright in 1983 [1], and was classified as low-grade B-cell non-Hodgkin's lymphoma that may involve a variety of extranodal sites. MALT lymphoma follows an indolent course, has a favorable prognosis,

and responds to various treatments, including chemotherapy and radiation. The most common site is the gastrointestinal tract; mainly the stomach, followed by salivary glands, respiratory tract, skin, soft tissue, breast, thyroid gland, thymus, ocular adnexa, and orbit [2–8]. MALT lymphomas may develop in the setting of chronic inflammatory disorders or autoimmune diseases, such as, chronic gastritis induced by *Helicobacter pylori* infection, lymphoepithelial sialoadenitis, lymphoid interstitial pneumonitis, Hashimoto thyroiditis, or Sjögren's syndrome [2,3,7,8].

Malignant lymphoma involving the salivary glands usually occurs secondary to high-grade, diffuse large B-cell lymphoma [9]. Primary lymphoma of the salivary glands is a rare entity that accounts for only 5% of all primary extranodal non-Hodgkin's lymphomas and 2% of all salivary gland tumors, and MALT lymphoma is the most prevalent histological subtype [9,10]. Although salivary glands do not normally contain MALT, they may acquire

^{*} Corresponding author. Tel.: +81 58 230 6439; fax: +81 58 230 6440.

E-mail addresses: hkato@gifu-u.ac.jp (H. Kato), masa-gif@umin.net (M. Kanematsu), hikichan-31129-gt-limone@r8.dion.ne.jp (H. Goto), kmizuta@gifu-u.ac.jp (K. Mizuta), aoki@gifu-u.ac.jp (M. Aoki), kuze-b@umin.ac.jp (B. Kuze), yhirose@gifu-

u.ac.jp (Y. Hirose).

Tel.: +81 58 230 6000; fax: +81 58 230 6080.

² Tel.: +81 58 231 2266; fax: +81 58 233 7772.

³ Tel.: +81 58 230 6439; fax: +81 58 230 6440.

lymphocytes as the result of a chronic inflammation induced, for example, by an autoimmune disorder. Salivary gland MALT lymphomas have affected parotid glands in 80% of reported cases and submandibular glands the remainder [9]. Most patients with salivary gland MALT lymphoma are in the sixth decade and multiple glands (often with bilateral involvement) are involved in approximately 10% of cases [10]. Patients present with a palpable mass, but pain or tenderness is observed in only a minority of cases.

Fine needle aspiration cytology is the only accurate investigation for classifying a parotid gland tumor as benign or malignant, but MR imaging is advocated for malignant tumors and for tumors expected to be in the deep lobe [11]. Although several authors have described the radiological imaging findings of salivary gland MALT lymphoma [2–6], the significances of MR findings, particularly of diffusion-weighted (DW) imaging, have yet to be determined. Here, we describe MR imaging findings including DW imaging and ¹⁸F-fluorodeoxyglucose (FDG) PET/CT findings in patients with MALT lymphoma of the salivary glands and discuss the diagnostic radiological clues of salivary gland MALT lymphoma.

2. Methods

2.1. Patients

The study was approved by the human research committee of our institutional review board, and complied with the guidelines of the Health Insurance Portability and Accountability Act. The requirement for informed consent was waived due to the retrospective nature of this study. The electronic medical chart system of Gifu University Hospital for patients with histopathologically proven MALT lymphoma of the salivary glands between July 2005 and February 2011 was searched and 10 consecutive patients (one man and 9 women; age range 58–73 years; mean 64.8 years) were identified. MR imaging was performed in all patients, CT in nine, and ¹⁸F-FDG PET/CT in eight, all within 3 months in individual patients.

2.2. MR imaging

All patients were examined using a 1.5-T MR imaging system (Intera Achieva 1.5 T Pulsar, Philips Medical Systems, the Netherlands in 6 patients and Gyroscan Intera 1.5 T, Philips Medical Systems, the Netherlands in the other 4); all MR images were obtained and reviewed in the transverse plane in a $20 \, \text{cm} \times 20 \, \text{cm} - 24 \, \text{cm} \times 24 \, \text{cm}$ field of view. T1-weighted spin-echo (TR/TE, $481-827/9-14 \, \text{ms}$; imaging matrices, $256 \times 256-512 \times 512$; slice thickness/intersectional gap, $4-5/1 \, \text{mm}$; no fat suppression) and T2-weighted fast spin-echo (TR/TE, $3381-4102/87-100 \, \text{ms}$; imaging matrices, $256 \times 256-512 \times 512$; slice thickness/intersectional gap, $4-5/1 \, \text{mm}$; no fat suppression) images were obtained for all patients. In five patients, gadolinium-enhanced non-fat-suppressed T1-weighted spin-echo images were obtained after the intravenous injection of 0.1 mmol/kg of gadopentetate dimeglumine (Magnevist, Schering, Berlin, Germany).

Six patients underwent DW imaging using a 1.5-T MR unit (Intera Achieva 1.5 T Pulsar) and a short-tau inversion recovery (STIR) single-shot spin-echo echo-planar imaging sequence (TR/TE/TI, 5490/72/170 ms; imaging matrices, 256 \times 256; field of view, 40 cm \times 40 cm; parallel imaging factor, 1.8; slice thickness/intersectional gap, 4/0 mm; slice number/data acquisition time, 36 slices/124s) with a b-value of 1000 s/mm². Motion-probing gradients were placed in the three orthogonal directions at the same strength.

An experienced neuroradiologist (11 years of post-training experience of head and neck imaging) reviewed all images for tumor numbers, locations, and sizes (average of perpendicular

long and short diameters). The reviewer also recorded the conventional MR signal intensities, intratumoral cystic formations, and ill-demarcated tumor margins. We also assessed signal intensities on DW images, and apparent diffusion coefficients (ADCs) were calculated using two b factors (0 and $1000 \, \text{s/mm}^2$). ADC values $[\times 10^{-3} \, \text{mm}^2/\text{s}]$ were measured on ADC maps placing a region of interest (ROI) over each lesion. ROIs were placed to encompass lesions as much as possible, while taking care to avoid cystic components and large vessels by referring to T2-weighted images.

2.3. CT imaging

CT imaging was performed in nine patients. An 8-slice CT (LightSpeed Ultra, GE Healthcare) with an $8 \times 2.5 \,\mathrm{mm}$ detector configuration was used in 5 patients, and for these, transverse unenhanced CT images were reconstructed using a 2.5-mm section thickness and no overlap. CT images of the remaining four patients were obtained by PET/CT.

2.4. ¹⁸F-fluorodeoxyglucose (FDG) PET/CT

In eight patients whole-body PET/CT imaging (Biograph Sensation 16, Siemens Medical Solutions, Malvern, PA) from the skull to the mid thigh was performed. Briefly, after at least 4h of fasting, patients received an intravenous injection of ¹⁸F-FDG (185 MBq). Blood glucose levels were checked in all patients before FDG injection, and no patient had a blood glucose level greater than 150 mg/dL. Approximately 60 min after FDG injection, CT and subsequent whole-body PET were performed.

The technical parameters of the 16-row multidetector CT system were; a gantry rotation speed of 0.5 s, a table speed of 24 mm per a gantry rotation, and quiet-breathing data acquisition. Transverse images were reconstructed using a 2.0-mm section thickness and no overlap. Neither oral nor intravenous contrast agent was administered at CT. The PET component had an axial view of 16.2 cm per bed position with an intersectional gap of 3.75 mm in one bed position, which necessitated data acquisition in six or seven bed positions. Axial PET images were obtained using an imaging matrix of 256×256 and a field of view of $50 \, \mathrm{cm} \times 50 \, \mathrm{cm}$.

For the semi-quantitative analysis of FDG uptake, the maximum standardized uptake value (SUVmax) of each lesion was measured by the same reviewer.

2.5. Statistical analysis

All statistical analyses were performed using SPSS version 18.0 (SPSS Inc, Chicago, IL). The unpaired t-test was used to compare the sizes of lesions with and without cystic formation. Pearson's rank correlation coefficients were calculated for relations between lesion sizes and ADC values and SUVmax.

3. Results

3.1. Patient characteristics

Patient characteristics are summarized in Table 1. There were one man and 8 women with ages ranging from 58 to 73 years (mean 64.8 ± 4.8 years). Clinical stages of lymphoma were stage I in three, stage II in five, and stage IV in two. Two patients suffered from Sjögren's syndrome and four from rheumatoid arthritis. All patients with rheumatoid arthritis had been treated through methotrexate. Blood test screening on admission revealed hepatitis C virus (HCV) infection in one patient (n = 8).

Download English Version:

https://daneshyari.com/en/article/6244525

Download Persian Version:

https://daneshyari.com/article/6244525

<u>Daneshyari.com</u>